

Statistical properties of metastable intermediates in DNA unzipping

J. M. Huguet,¹ N. Forns,^{1,2} and F. Ritort^{1,2,*}

¹*Departament de Física Fonamental, Facultat de Física, Universitat de Barcelona, Diagonal 647, 08028 Barcelona, Spain*

²*CIBER-BBN, Networking Centre on Bioengineering, Biomaterials and Nanomedicine, ISCIII, Spain*

We unzip DNA molecules using optical tweezers and determine the sizes of the cooperatively unzipping and zipping regions separating consecutive metastable intermediates along the unzipping pathway. Sizes are found to be distributed following a power law, ranging from one base pair up to more than a hundred base pairs. We find that a large fraction of unzipping regions smaller than 10 bp are seldom detected because of the high compliance of the released single stranded DNA. We show how the compliance of a single nucleotide sets a limit value around 0.1 N/m for the stiffness of any local force probe aiming to discriminate one base pair at a time in DNA unzipping experiments.

PACS numbers: 87.15.-v, 82.37.Rs, 82.39.Pj, 87.80.Nj

The mechanical response of biomolecules to externally applied forces allows us to investigate molecular free energy landscapes with unprecedented accuracy. Single molecule experiments with optical tweezers, atomic force microscope (AFM), and magnetic tweezers are capable of measuring forces in the pN range and energies as small as tenths of kcal/mol. An experiment that nicely illustrates the potential applications of single molecule manipulation is molecular unzipping [1–5]. By applying mechanical force to the ends of biopolymers such as DNA, RNA, and proteins, it is possible to break the bonds that hold the native structure and measure free energies and kinetic rates. In unzipping experiments, a DNA double helix is split into two single strands by pulling them apart and the force vs. distance curve (FDC) measured. A typical FDC shows a force plateau around 15 pN with a characteristic sawtooth pattern corresponding to the progressive separation of the two strands. Mechanical unzipping is also a process mimicked by motor proteins that unwind the double helix. In fact, anticorrelations between unzipping forces and unwinding rates have been found in DNA helicases suggesting that such enzymes unzip DNA by exerting local stress [6]. DNA unzipping experiments have several applications such as identifying specific locations at which proteins and enzymes bind to the DNA [5]. Moreover, the strong dependence of the shape of the sawtooth pattern with the sequence might be used for DNA sequencing [7], i.e., a way to infer the DNA sequence from the unzipping data. A limitation factor in these applications is the accuracy at which base pair (bp) locations along the DNA can be resolved. This is mainly determined by the combined stiffness of the force probe and the large compliance of the released single stranded DNA (ssDNA) [1, 8]. The unzipping process, even if carried out reversibly (i.e., infinitely slowly), shows a progression of cooperative unzipping-zipping transitions that involve groups of bps of different sizes. These cooperatively unzipping-zipping transitions regions (CUR) of bps breath in an all-or-none fashion hindering details about the individual bps participating in such transitions. Unzipping experiments pose challenging questions to the ex-

perimentalist and the theorist. What is the typical size of these CUR? What is the smallest size of the CUR that can be detected with single molecule techniques? Under what experimental conditions might be possible to resolve large CUR into individual bps? There have been several DNA unzipping studies with controlled force using magnetic tweezers. Because at constant force the unzipping transition is abrupt, this setup is not suitable to answer such questions [3, 9].

We carried out DNA unzipping experiments with optical tweezers [10, 11] and determined the distribution of CUR sizes in DNA fragments a few kbp long. For the experiments, a 2.2 kbp DNA molecular construct was synthesized [11]. In a typical unzipping experiment one bead is held fixed at the tip of a micropipette and the other bead is optically trapped and the force exerted on the molecule measured. By moving the center of the optical trap at a very low speed (10 nm/s) double stranded DNA (dsDNA) is progressively and quasireversibly converted into ssDNA through a succession of intermediate states corresponding to the successive opening of CUR (Fig. 1a). The experimentally measured FDC shows a sawtoothlike pattern (Fig. 1b) that alternates force rips and gentle slopes. Slopes correspond to the elastic response of the molecule while the force rips correspond to the release of CUR. The slope is due to the combined elastic response of the optical trap and the released ssDNA. The size of a CUR can be inferred from the difference of slopes that precede and follow a given force rip. However, the identification of the CUR sizes is not straightforward as often the slopes cannot be isolated because the experimental FDC exhibits noise. Here we extract the different sizes of the CUR that separate contiguous intermediate states along the unzipping pathway. For that we adopt a Bayesian approach where for each experimental data point (distance, force) we determine the most probable intermediate state to which the data point belongs.

To this end we consider the molecular system as composed of different elements: the optical trap, the dsDNA handles, the released ssDNA and the hairpin at the intermediate state I_n where n bases are open. We express the

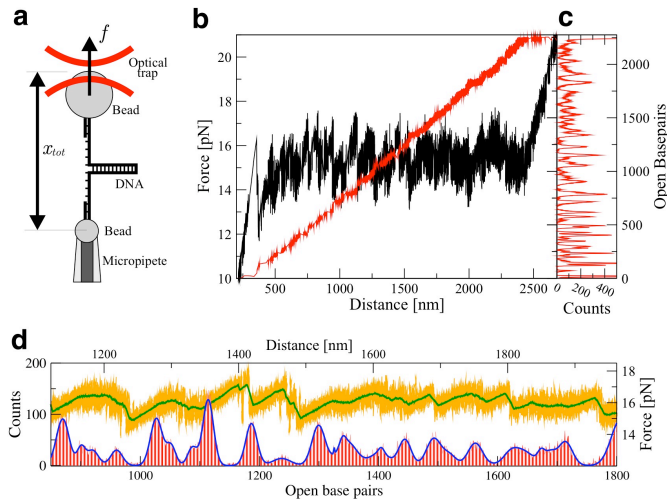


FIG. 1: (color online). Identifying CUR in DNA unzipping experiments. **(a)** Experimental setup. A 2.2 kbp sequence of DNA is unzipped using an optical trap and a micropipette. **(b)** Black curve shows the raw data of a typical FDC in an unzipping experiment. Red or gray curve shows the number of open bps n^* corresponding to each experimental data point (y axis of this curve is shown in panel c). **(c)** Histogram of the values for n^* shown in panel b. **(d)** The lower curve shows a detailed view of the histogram overlapped with a fit to a sum of Gaussians. The upper curve shows the FDC (raw data and 1 Hz low pass filtered data) corresponding to that region of the histogram.

total distance between trap and pipette x_{tot} at a given force f as the sum of the extensions of each element at that force:

$$x_{\text{tot}}(f, n) = x_b(f) + x_h(f) + x_s(f, n) + \frac{\phi_b}{2} \quad (1)$$

where x_b is the position of the bead with respect to the center of the optical trap; x_h is the extension of the flanking dsDNA handles; x_s is the extension of the released ssDNA and ϕ_b is the diameter of the bead. The extension of the ssDNA depends on the number of open bases at the intermediate state I_n . The different contributions to Eq. (1) are calculated by using well-known elastic models for biopolymers [11]. For each experimental data point of the FDC (x, f), the intermediate state I_{n^*} that passes closest to that point for a fixed force f is determined by

$$|x - x_{\text{tot}}(n^*, f)| = \min_n (|x - x_{\text{tot}}(n, f)|). \quad (2)$$

In this way each experimental data point (x, f) is associated to a value of n^* (red or gray curve in Fig. 1b). The histogram built from all values n^* results in a series of sharp peaks that can be identified with the many intermediate states I_n (Fig. 1c). The histogram contains information about the stability of the intermediate states: the higher the peak, the higher the stability of that state and the larger the GC content of that part of the sequence

(data not shown). The histogram can be fit to a sum of Gaussians each one characterized by its mean, variance and statistical weight (Figs. 1d and 2a). Finally, the size of the CUR is obtained by calculating the difference of the means (in bps) between consecutive Gaussians. The experimental distribution of CUR sizes is shown in Fig. 2b. Sizes range from a few bps up to 90 bp with a maximum number of detected CUR sizes between 20 and 50 bp.

To better understand the distribution of CUR sizes we have computed the sequence dependent free energy profile using a mesoscopic model for DNA based on nearest neighbour bp interactions that includes the different elements of the experimental setup [12, 13]. The model is defined by the total free energy of the system, $G(x_{\text{tot}})$, which gets contributions from the partial free energies $G(x_{\text{tot}}, n)$ of the many intermediates I_n : $G(x_{\text{tot}}) = -k_B T \log\{\sum_n \exp[-G(x_{\text{tot}}, n)/k_B T]\}$. From $G(x_{\text{tot}})$ we can determine the theoretical FDC by using the relation, $f(x_{\text{tot}}) = \frac{\partial G(x_{\text{tot}})}{\partial x_{\text{tot}}}$. We have used this model to compute the partial free energies $G(x_{\text{tot}}, n)$ of all intermediates I_n . For a given value of x_{tot} we identify the

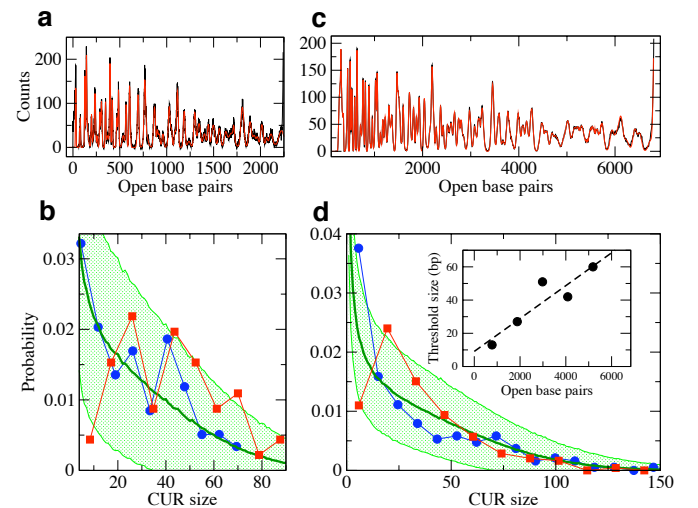


FIG. 2: (color online). CUR size distributions. **(a)** Histogram of n^* values corresponding to the different intermediate states for the 2.2 kbp DNA sequence. Red or gray curve shows the experimentally measured histogram. Black curve shows the fit to a sum of Gaussians. **(b)** Distribution of CUR sizes for the 2.2 kbp sequence. Red or gray curve shows the experimentally measured distribution. Blue or dark gray curve shows the distribution predicted by the mesoscopic model for DNA. Green or smooth and thick curve shows the distribution predicted by the toy model (see text) and the shaded area shows the standard deviation from different sequence realizations of the same length. **(c)** Histogram of intermediate states for the 6.8 kbp sequence. Same color code as in panel a. **(d)** Distribution of CUR sizes for the 6.8 kbp sequence. Same color code as in panel b. **(Inset of d)** Threshold size n^{thr} as a function of the number of open bps n . The dashed line is a linear fit, $n^{\text{thr}} = 9.1 + 0.01n$. For both molecular constructs, 6 molecules have been measured and analyzed.

most stable intermediate I_{n^*} corresponding to the value of n^* for which $G(x_{\text{tot}}, n)$ is the absolute minimum [i.e., $G(x_{\text{tot}}, n^*) \leq G(x_{\text{tot}}, n), \forall n$]. Integer values of n^* change in a stepwise manner as x_{tot} is continuously varied according to the following scheme

$$\dots \Leftrightarrow I_{n_a^*} \Leftrightarrow I_{n_b^*} \Leftrightarrow I_{n_c^*} \Leftrightarrow \dots \quad (3)$$

where n_a^* , n_b^* , n_c^* indicate the number of open bps corresponding to consecutive intermediates. Differences between consecutive values of n^* provide the sizes of the CUR. The resulting size distributions are shown in Fig. 2b. The good agreement between the experimental and the theoretical size distributions shows that our method of analysis is capable of discriminating the metastable intermediates during unzipping. There are two remarkable facts in Fig. 2b. First, the mesoscopic model predicts a large fraction of CUR of size smaller than 10 bp that are not experimentally observed. Second, size distributions are not smooth but have a rough shape in agreement with the prediction by the mesoscopic model. In order to check the generality of these results we have repeated the same analysis by unzipping a different and longer molecular construct of 6.8 kbp (Figs. 2c, 2d). The agreement between experiments and theory remains good. Again a large fraction of predicted CUR sizes smaller than 10 bp are not detected [11]. However, the CUR size distributions are now smoother suggesting that a monotonically decreasing continuous distribution could describe the distribution of CUR in the thermodynamic (infinite DNA length) limit. The fact that CUR sizes show a long tailed distribution indicates that large sizes occur with finite probability. However, large-sized CUR hinder their internal DNA sequence limiting the possibility of sequencing DNA by mechanical unzipping. Under what experimental conditions is it possible to break up large-sized CUR into individual bps?

In order to answer this question we have developed a toy model useful to elucidate the mathematical form of the CUR size distribution. Similar distributions have been investigated in the context of DNA thermal denaturation [14, 15] and DNA unzipping experiments in the constant force ensemble [9]. Our model contains only two elements: the bead in the optical trap and the DNA construct to be unzipped. The latter is composed of the DNA duplex and the released ssDNA (Fig. 3a). The optical trap is modeled by a harmonic spring with energy, $E_b(x_b) = \frac{1}{2}kx_b^2$. The DNA duplex is modeled as a one-dimensional random model with bp free energies ϵ_i along the sequence [16]. The free energy of a given intermediate I_n is given by $G_{\text{DNA}}(n) = -\sum_{i=1}^n \epsilon_i$. The ϵ_i are distributed according to a normal distribution $\mathcal{N}(\mu, \sigma)$, where $\mu (< 0)$ and σ are the mean and the standard deviation of the energies, respectively (other more realistic energy distributions give similar results). The released ssDNA is taken as inextensible: its extension (x_m) is given by $x_m = 2dn$, where d is the interphosphate dis-

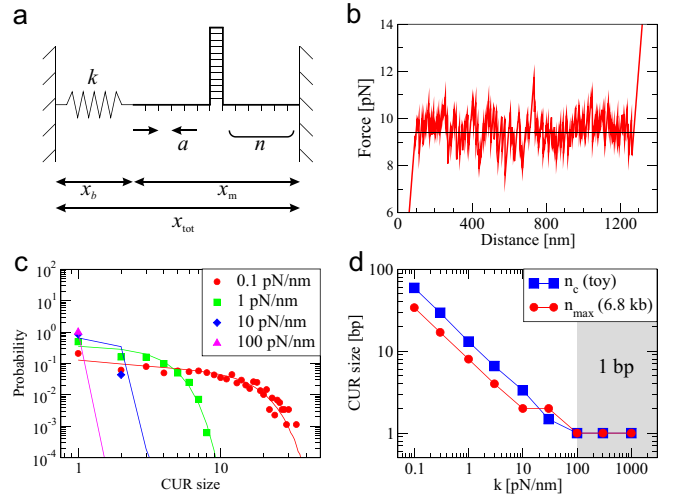


FIG. 3: (color online) Toy model. (a) The unzipping experiment is modeled with the minimum elements of the experimental setup. (b) Red or gray curve shows the FDC for one random realization. The horizontal black line shows the analytical approximation when disorder is neglected. (c) CUR size distributions in log-log scale for some values of k using the toy model. Data plotted with points shows the CUR size distribution for the 6.8 kbp sequence. Data plotted with lines, shows the average CUR size distribution over 10^4 realizations ($k=60$ pN/ μm , $d = 0.59$ nm, $\mu=-1.6$ kcal/mol, $\sigma=0.5$ kcal/mol). (d) The fit of the average CUR size distributions in panel c to Eq. 6 give the cutoff size n_c . It decreases like $n_c \simeq k^{-2/3}$. Blue or dark gray curve shows n_c vs k . Red or gray curve shows the maximum CUR size (n_{max}) predicted by the toy model for the 6.8 kbp sequence. For $k > 100$ pN/nm, both curves level off to CUR sizes of 1 bp.

tance, n is the number of open bps, and the factor 2 stands for the two strands of ssDNA. By using the relation $x_b = x_{\text{tot}} - 2dn$ (Fig. 3a), the total energy of the system can be written as

$$E(x_{\text{tot}}, n) = \frac{1}{2}k(x_{\text{tot}} - 2dn)^2 - \sum_i^n \epsilon_i. \quad (4)$$

At fixed x_{tot} , the system will occupy the state (n^*) that minimizes the total energy of the system, i.e., $E(x_{\text{tot}}, n^*) \leq E(x_{\text{tot}}, n), \forall n$. The function $n^*(x_{\text{tot}})$ gives the thermodynamic energy function at the minimum, $E_m(x_{\text{tot}})$, and the FDC, $f(x_{\text{tot}}) = \frac{\partial E_m(x_{\text{tot}})}{\partial x_{\text{tot}}}$. The FDC obtained from this model reproduces the sawtooth pattern that is experimentally observed (Fig. 3b).

Equation 4 can be approximated by neglecting the disorder and taking $\epsilon_i = \mu, \forall i$. This gives,

$$E(x_{\text{tot}}, n) \simeq \frac{1}{2}k(x_{\text{tot}} - 2dn)^2 - \mu n. \quad (5)$$

From this approximation we immediately get the following results $n^*(x_{\text{tot}}) = \frac{1}{2d}(x_{\text{tot}} + \frac{\mu}{2dk})$, $E_m(x_{\text{tot}}) =$

$-\frac{\mu}{2d}(x_{\text{tot}} + \frac{\mu}{4kd})$, and $f_m = -\frac{\mu}{2d}$. These expressions capture the dependence of the averaged number of open bps, energy, and force on the external parameters μ, σ [11].

Finally we have numerically computed the CUR size distribution. We find that this mostly depends on σ and k . For several combinations of σ and k we simulated 10^4 realizations (i.e., sequences) of 10^4 bp sequences, while d and μ were kept constant. The size distributions are excellently fit by a power law with a superexponential cutoff [11]:

$$P(n) = An^{-B} \exp(-n/n_c)^C, \quad (6)$$

where $P(n)$ is the probability of observing a CUR of size n ; A, B, C and n_c (cutoff size) are positive fitting parameters. How much can the toy model predict the experimental results? For the 2.2 kbp sequence the parameters that best fit the experimental histograms are $\mu = -2.80$ kcal/mol, $\sigma = 2.2$ kcal/mol and $k = 60$ pN/ μm (equal to the stiffness of the trap that we can measure independently). This gives $A = 0.058, B = 0.42, C = 2.95$, and $n_c = 69$ (fit shown in Fig. 2b). For the 6.8 kbp sequence we find $\sigma = 3.3$ kcal/mol while k and μ have the same value. This gives $A = 0.050, B = 0.43, C = 3.0$, and $n_c = 91$ (fit shown in Fig. 2d). The values of μ and σ are not far from the actual mean and standard deviation of the energies of the nearest neighbour model for DNA, $\mu = -1.6$ kcal/mol, $\sigma = 0.44$ kcal/mol [16]. Having not included the elastic effects of the ssDNA in the toy model we should not expect a good match between the fitting and the experimental values.

What is the limiting factor in detecting small-sized CUR? A look at Figs. 1c,2a,2c, and Figs. S14 and S15 in [11] shows that histograms become smoother as the molecule is progressively unzipped. The increased compliance of the molecular setup as ssDNA is released markedly decreases the resolution in discriminating intermediates. In fact, for the 6.8 kbp construct we found that along the first 1500 bp of the hairpin only 30% of the total number CUR smaller than 10 bp are detected whereas beyond that limit no CUR smaller than that size is discriminated. If we define the threshold size n^{thr} as the size of the CUR above which 50% of the predicted CUR are experimentally detected we find that n^{thr} increases linearly with the number of open bps putting a limit around 10 bp for the smallest CUR size that we can detect (Fig. 2d, inset). What is the limiting factor in resolving large-sized CUR into single bps? Only by applying local force on the opening fork (thereby avoiding the large compliance of the molecular setup) and by increasing the stiffness of the probe might be possible to shrink CUR size distributions down to a single bp [8]. Figures 3c and 3d show how the CUR size distributions shrink and the largest CUR size decreases as the stiffness increases. Its value should be around 50-100 pN/nm for all CUR sizes to collapse into a single bp. Remarkably enough this number is close to the stiffness value expected

for an individual DNA nucleotide stretched at the unzipping force [11]. Any probe more rigid than that will not do better. Similarly to the problem of atomic friction between AFM tips and surfaces we can define a parameter η (defined as the ratio between the rigidities of substrate and cantilever) that controls the transition from stick slip to continuous motion [17]. For DNA unzipping we have $\eta = \frac{|\mu|}{kd^2}$ where μ is the average free energy of formation of a single bp, k is the probe stiffness, and d is the interphosphate distance. The value $\eta = 1$ determines the boundary where all CUR are of size equal to one bp ($\eta < 1$). In our experiments we have $\eta \simeq 500$ and to reach the boundary limit $\eta = 1$ we should have $k \sim 100$ pN/nm consistently with what is shown in Figs 3c and 3d. It is remarkable that the elastic properties of ssDNA lie just at the boundary to allow for one bp discrimination. This suggests that molecular motors that mechanically unwind DNA can locally access the genetic information one bp at a time [11].

In summary, we have measured the distribution of sizes of unzipping regions of DNA. A toy model reproduces the experimental results and can be used to infer the experimental conditions under which the unzipping is done one bp at a time. This is achieved when the stiffness of the probe is higher than 100 pN/nm, which coincides with the stiffness of one base of ssDNA at the unzipping force.

J.M.H. acknowledges a grant from the Ministerio de Educación y Ciencia in Spain. F.R. is supported by grants No. FIS2007-3454 and No. HFSP (RGP55-2008).

* To whom correspondence should be addressed.

fritort@gmail.com; <http://www.ffn.ub.es/ritort/>

- [1] U. Bockelmann *et al.*, *Biophys. J.* **82**, 1537 (2002).
- [2] M.T. Woodside *et al.*, *Science* **314**, 1001 (2006).
- [3] C. Danilowicz *et al.*, *Proc. Natl. Acad. Sci. U.S.A.* **100**, 1694 (2003).
- [4] M. Rief, H. Clausen-Schaumann, and H. E. Gaub, *Nat. Struct. Biol.* **6**, 346 (1999).
- [5] S.J. Koch *et al.*, *Biophys. J.* **83**, 1098 (2002).
- [6] D. S. Johnson *et al.*, *Cell* **129**, 1299 (2007).
- [7] V. Balducci *et al.*, *Phys. Rev. Lett.* **96**, 128102 (2006).
- [8] N. K. Voulgarakis *et al.*, *Nano Lett.* **6**, 1483 (2006).
- [9] D. K. Lubensky and D. R. Nelson, *Phys. Rev. E.* **65**, 031917 (2002).
- [10] Experiments were done in a dual-beam miniaturized optical tweezers with fiber-coupled diode lasers (845 nm wavelength) that produce a piezocontrolled movable optical trap and measure force using conservation of light momentum. The experimental setup is based on C. Bustamante and S. B. Smith, U.S. Patent No. 7 133 132 B2 (2006).
- [11] See Supplementary Information for the appendices.
- [12] M. Manosas and F. Ritort, *Biophys. J.* **88**, 3224 (2005).
- [13] M. Manosas *et al.*, *Biophys. J.* **92**, 3010 (2007).
- [14] S. Ares and G. Kalosakas, *Nano Lett.* **7**, 307 (2007).
- [15] T. Ambjörnsson *et al.*, *Phys. Rev. Lett.* **97**, 128105 (2006); *Biophys. J.* **92**, 2674 (2007).
- [16] J.J. SantaLucia, *Proc. Natl. Acad. Sci. U.S.A.* **95**, 1460 (1998).
- [17] A. Socoliuc *et al.*, *Phys. Rev. Lett.* **92**, 134301 (2004).

Supplementary information of the paper

Statistical properties of metastable intermediates in DNA unzipping

J. M. Huguet

*Departament de Física Fonamental, Facultat de Física,
Universitat de Barcelona, Diagonal 647, E-08028, Barcelona*

N. Forns and F. Ritort*

*Departament de Física Fonamental,
Facultat de Física, Universitat de Barcelona,
Diagonal 647, E-08028, Barcelona and
CIBER de Bioingeniería, Biomateriales y Nanomedicina,
Instituto de Salud Carlos III, Madrid*

(Dated: 10 December 2009)

arXiv:1010.1169v1 [physics.bio-ph] 6 Oct 2010

*To whom correspondence should be addressed: fritort@gmail.com; <http://www.ffn.ub.es/ritort/>

Contents

1. Experimental details	3
1.1. DNA sequences	3
1.2. Measurements calibration and data acquisition	3
1.3. Statistics and reproducibility of measurements	4
2. Experimental errors	4
2.1. Parameters used in the model	4
2.2. About using force-distance curves (FDCs) instead of force-extension curves (FECs)	6
2.3. Base pair determination	7
2.4. Reproducibility of intermediate histograms	8
2.5. Error in CUR size distributions	8
2.6. Discrepancies between experimental and theoretical CUR size distributions	9
3. The toy model	10
3.1. Approximated solution to the toy model	10
3.2. Size distribution of CUR	11
3.2.1. Dependence on σ	12
3.2.2. Dependence on k	12
4. Stiffness of one nucleotide	14
5. Protein-DNA interaction	15
6. CUR and genes	16
References	17

1. EXPERIMENTAL DETAILS

1.1. DNA sequences

The two DNAs (2.2 and 6.8 kb) unzipped in the experiments are obtained by gel extraction from λ -DNA. They are synthesized following similar procedures: 1) A restriction enzyme is used to cleave the λ -DNA molecule. The SphI restriction enzyme (BamHI) is used for the 2.2 kb (6.8 kb) sequence. 2) A fragment of 2216 bp (6770 bp) is isolated from the resulting digestion by gel extraction. 3) Two handles of 29 bp are added by hybridization and annealing of short complementary oligonucleotides to one end of the 2.2 kb (6.8 kb) fragment. Another oligonucleotide that forms a tetraloop (5'-acta-3') is also annealed at the other end of the 2.2 kb (6.8 kb) fragment. The handles were labeled with biotin and digoxigenin that specifically attach to coated polystyrene beads. Figure S1 shows the resulting sequences. Experiments were done in aqueous buffer containing 10 mM Tris-HCl (pH 7.5), 1 mM EDTA, 500 mM NaCl and 0.01% Sodium Azide.

1.2. Measurements calibration and data acquisition

The instrument has a force resolution below 1 pN, which represents about 6% uncertainty at the mean unzipping force (16.5 pN). The force is inferred by measuring the deflection of the scattered light by the bead. The offset of the deflected light is measured using a Position Sensitive Detector (PSD), which is converted into force by multiplying it with a calibration factor. The force is calibrated using three different methods and all agree within the aforementioned uncertainty: power spectrum measurements, the Stokes law and the equipartition theorem. The distance measurements have a resolution of 1 nm which represents about 3%. The distance is measured with a light-lever. A small amount of the laser beam is split before it enters the focusing objective and forms the optical trap. The light is redirected to a Position Sensitive Detector (PSD) that measures the position of the center of the optical trap. The PSD is calibrated using a motorized stage with known pitch distance.

The analog signals from the PSDs (position and force) are filtered using an analog low pass filter of bandwidth 1 kHz. The resulting signal is sampled at 4 kHz producing the raw data that we obtain in the unzipping experiment.

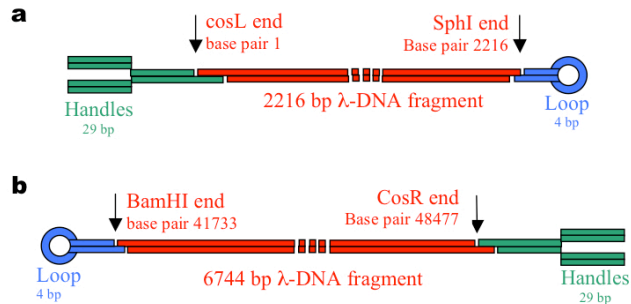


FIG. S1: DNA molecules unzipped. **a.** The 2.2 kb sequence. The main sequence (in red) corresponds to the bases from 1 to 2216 of the λ genome. The handles are annealed at the cosL end and the molecule is unzipped from 5' to 3' direction. The linking fragment (duplex of DNA in green) between the handles and the main sequence is 5'-aatagagacacatatataatagatctt-3'. The linking fragment (duplex of DNA in blue) between the main sequence and the loop is 5' tgatagcct-3'. **b.** The 6.8 kb sequence. The main sequence (in red) corresponds to the bases from 41733 to 48477 of the λ genome. The handles are annealed at the cosR end and the molecule is unzipped along the 3' to 5' direction. The fragment between the main sequence and the handles is 5'-gggcggcgacctaagatctattatatatgtgtctctatt-3'. The fragment between the loop and the main sequence is 5'-aatagagacacatatataatagatctt-3'.

1.3. Statistics and reproducibility of measurements

Six different molecules were analyzed for the 2.2 kb and the 6.8 kb DNA sequences.

In fig S2 we show force-distance curves measured for 3 different molecules corresponding to the 2.2 kb and 6.8 kb sequences. As can be seen our measurements are reproducible. Slight differences between different traces are due to the variability of the molecular setup and instrumental drift effects.

2. EXPERIMENTAL ERRORS

2.1. Parameters used in the model

Here we give the numerical values of the parameters used in the model (Eq. (1) main text) to extract the histogram of intermediate states. The bead in the optical trap is modeled by

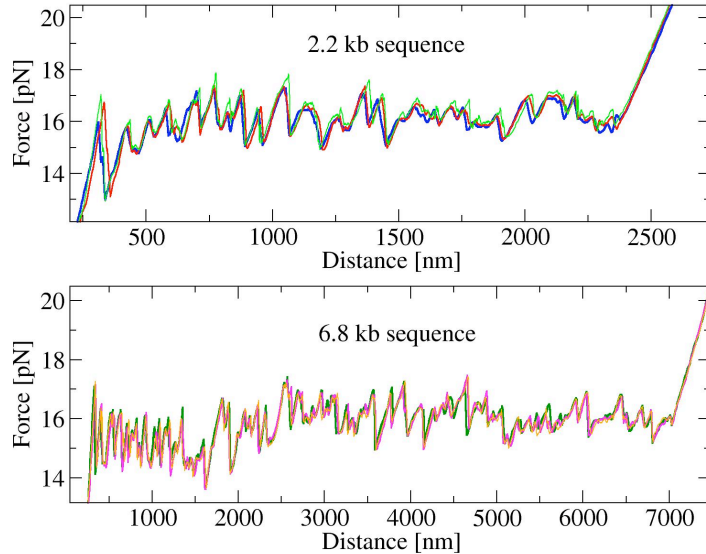


FIG. S2: Experimental FDC of 3 molecules corresponding to the 2.2 kb sequence (upper panel) and the 6.8 kb sequence (lower panel). Since the raw data is too noisy, the data has been filtered with a low-pass running-average filter with a bandwidth of 1 Hz to clearly see the traces.

a Hookean spring, $f = kx_b$, where k is the measured stiffness of the optical trap and x_b is the position of the bead with respect to the center of the optical trap. The measured stiffness of the optical trap is $k = 60 \pm 5$ pN/nm (error is due to bead size heterogeneity). The elastic response of the handles is described by the worm-like chain (WLC) model and parameters are obtained from the literature [1]. The elastic response of the released ssDNA is described using a freely-jointed chain (FJC) model [2]. We use $d = 0.59$ nm for the ssDNA because this value fits well the elastic response of the ssDNA in our data. This value is similar to the one found by Dessinges et al. [3] ($d=0.57$ nm at 1 and 10 mM phosphate buffer) and to Johnson et al. [4] ($d=0.537$ nm at 50 mM NaCl, 20 mM Tris-HCl, pH 7.5). Moreover we consider that interphosphate distance is an effective parameter of an elastic model which does not need to be equal to the parameter measured by crystallography. In order to determine the Kuhn length of the ssDNA, we have proceeded as follows (see fig S3): We fix the interphosphate distance at $d=0.59$ nm and then we determine the Kuhn length of the ssDNA by fitting the last part of the FDC (where the dsDNA duplex is fully unzipped and the elastic response of the ssDNA can be measured) to a Freely Jointed Chain. The best value among the 12 molecules (6 molecules of each) for the Kuhn length is $b = 1.2 \pm 0.3$ nm. We assume an inextensible Freely Jointed Chain model because the effect of a stretch modulus on the elastic

response of the ssDNA is barely negligible below 20 pN, where the unzipping is observed.

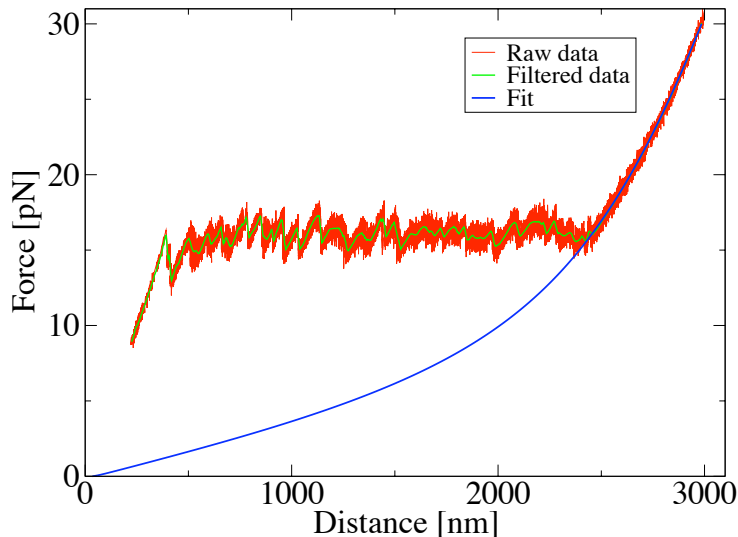


FIG. S3: Fit of the Kuhn length of the ssDNA using the last part of the FDC to one 2.2 kb molecule.

2.2. About using force-distance curves (FDCs) instead of force-extension curves (FECs)

We define the distance x_{tot} as the length between the bead of the micropipette and the center of the optical trap (see Fig. 1a for an illustration of how x_{tot} is defined and Eq. (1) for a mathematical expression). This magnitude is a measurement that we collect directly from the instrument as the optical trap is moved up and down along the fluidics chamber. This is the control parameter in the experiment, i.e. the variable that does not fluctuate and the parameter that determines the statistical ensemble (what we call mixed ensemble). Since we know the trap stiffness (k) and we measure the total distance (x_{tot}) and the force (f), it is straightforward to convert the force-distance curve into a force-extension curve using the following relation: $x_m = x_{tot} - f/x_b$, where x_m is the molecular extension. As we show in the figure S4 we do not appreciate any significant difference when computing the histogram using a FEC or a FDC.

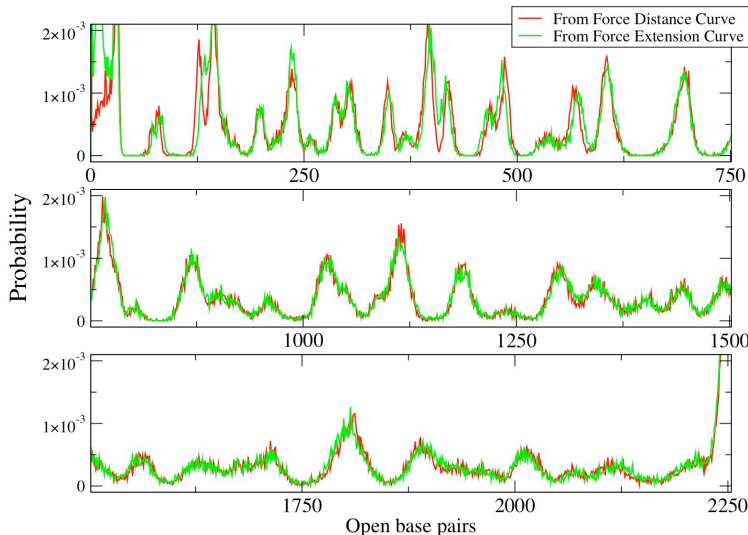


FIG. S4: Histograms of intermediate states calculated using the FDC and the FEC. Note that, apart from some peaks in the beginning, there are no significant differences in the position of the peaks. Eventually, the distribution of CUR sizes will hardly be affected by the choice of FDC or FEC.

2.3. Base pair determination

Here we will discuss what level of uncertainty is introduced in calculating the number of base pairs unzipped through the use of model parameters. The contribution of the handles can be neglected as they behave almost like rigid rods (their contour length is much shorter than the persistence length). We have calculated the same histograms varying the Kuhn length of the ssDNA. When the Kuhn length is modified, the peaks of the histogram are located in a different position. The error introduced might be as large as ~ 60 bp when the Kuhn length is varied from 1.2 nm to 1.5 nm. However, the difference between the position of two correlative peaks is weakly affected by the Kuhn length (~ 3 bp). Fig. S5 illustrates these results. Finally, we do not expect important differences in the determination of the CUR sizes by using a slightly different value of the interphosphate distance d because a correction in that value is somehow equivalent to a change in the value of the Kuhn length.

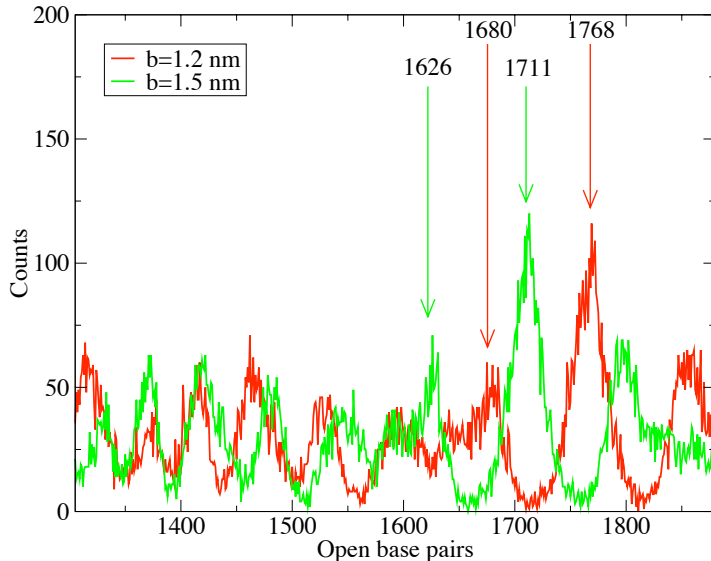


FIG. S5: Dependence of the histogram on the model parameters. Here we show a region of two histograms of intermediate states that have been calculated using different values of the Kuhn length (b) for the ssDNA (see Eq. (1) in the main text). We highlight two peaks (green and red arrows) of each histogram that correspond to two consecutive intermediate states. The error in the CUR size due to the Kuhn length is less than 4% (about 3 bps error in a 80 bp-sized CUR).

2.4. Reproducibility of intermediate histograms

Histograms in fig S6 show the probability of intermediate states for the 6 different molecules of 6.8 kb (each molecule corresponds to one color). Despite of the fact they look very similar, there are some differences at the beginning (between 0 and 650 bp), mainly due to two reasons: 1) Molecular frying. Some molecules are not capable of completely refold into the DNA duplex and sometimes the first 50-100 bases of the stem remain open. 2) Adhesion between the two beads. The two beads must be very close each other when the DNA is fully zipped because the handles of the molecular construct are very short. Sometimes the beads get stuck and the firsts rips of the unzipping curve cannot be detected.

2.5. Error in CUR size distributions

The experimental error of CUR size distributions is negligible as intermediate histograms are fully reproducible among different molecules (see fig. S6). However we can estimate

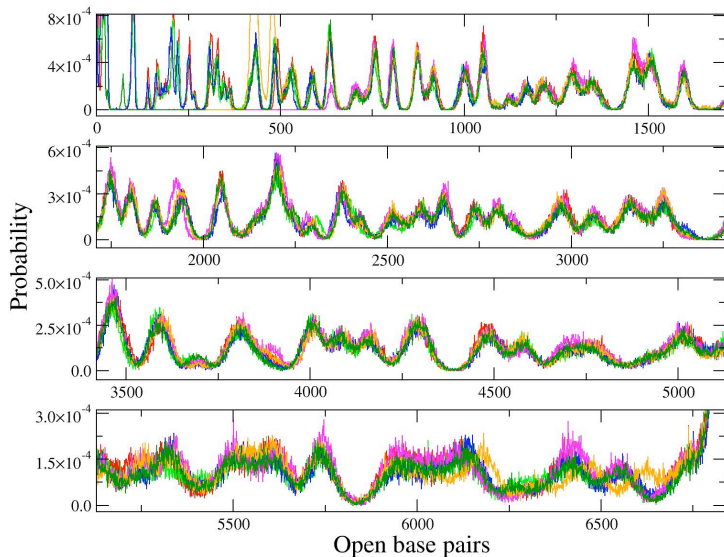


FIG. S6: Histograms of intermediate states for six different molecules of 6.8 kb. They are depicted in red, green, blue, magenta, orange and dark green. Although the height of each peak is different for the six histograms, the position of the peak is almost the same (± 10 bp). The histograms for the 2.2 kb molecules have similar reproducibility.

the error committed in measuring the CUR size distribution among different sequence realizations of the same DNA length. Although that error should vanish for infinitely long sequences (CUR size distributions are self-averaging in the thermodynamic limit) there are large fluctuations for finite length molecules. An experimental measurement of unzipping curves for many DNA sequences is beyond our capabilities. However to estimate that error we can use the toy model to determine the expected standard deviation of the CUR size distributions (see Fig. S7).

2.6. Discrepancies between experimental and theoretical CUR size distributions

Discrepancies between the experimental results and the mesoscopic model are attributed to two factors: 1) Small CUR are missed due to limited instrumental resolution as described in the paper; 2) Medium and large CUR sizes are prone to large error because less than 10 bp CUR are seldom detected. Indeed, the power law describing the CUR size distributions indicates that the majority of CUR is small sized. However if one small sized CUR is missed then medium or large sized CUR will be overcounted as they should split into smaller pieces

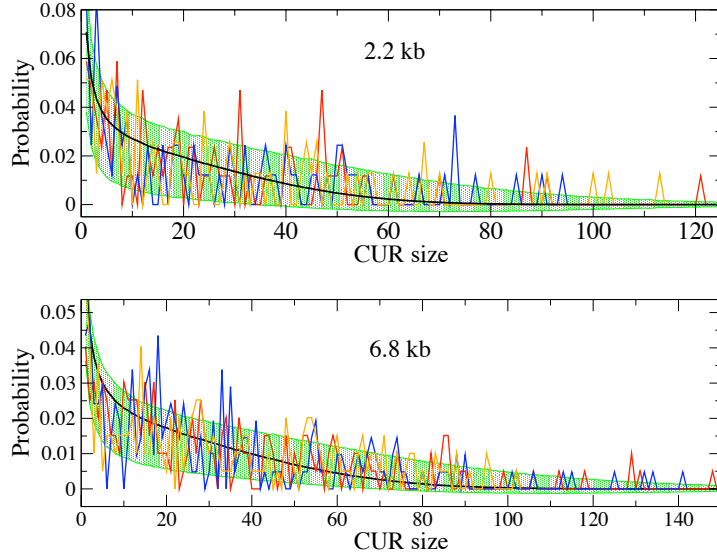


FIG. S7: CUR size distributions calculated with the toy model. Upper (lower) panel shows the results for a 2252 (6838 kb) sequence. The black curve shows CUR size distribution averaged over 10^4 realizations. The green region represents the upper and lower limits of the error bars that correspond to the standard deviation of those realizations. Red, blue and orange curves show 3 different realizations. Note the large deviations from the average histogram due to the finite length of the sequences.

whenever they contain a small CUR. It is a difficult math problem to evaluate the final effect of all missed CUR in the resulting CUR size histogram. These two effects concur to modify the shape of the power law for the 6.8kb molecule in Fig. 2d. Yet it is remarkable that the general trend of the experimental data shown in Figs. 2c and 2d follows reasonably well the predictions of the mesoscopic model. This is specially true for the 2.2 kb data shown in Fig. 2b where the non-monotonic oscillations observed in the experimental distribution are captured by the mesoscopic model.

3. THE TOY MODEL

3.1. Approximated solution to the toy model

The toy model (Eq. (4) in the main text) gathers all the relevant features of a DNA unzipping experiment. The most interesting of them are the force rips in the FDC and

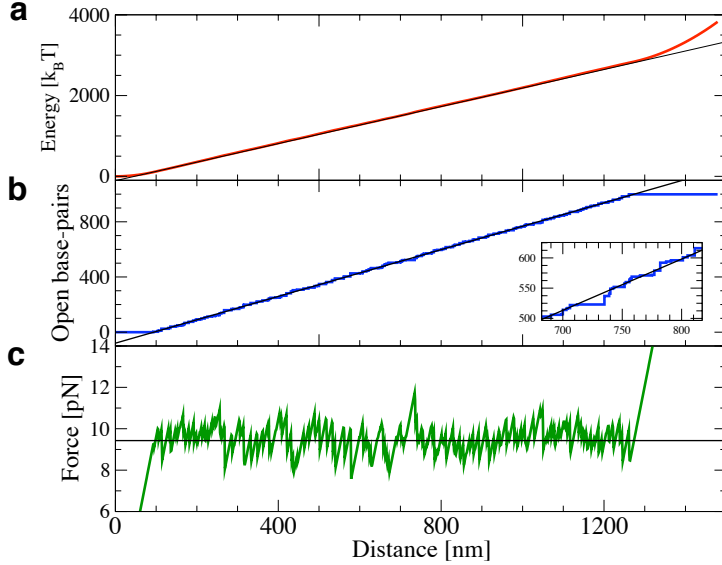


FIG. S8: Average behavior and one realization of the toy model. Black curves in all the panels show the approximated solution (see main text for the expressions) and colored curves show the solution for one disorder realization. The following parameters have been used: $k=60$ pN/ μm , $d=0.59$ nm, $\mu=-1.6$ kcal/mol, $\sigma=3.20$ kcal/mol. **(a)** Energy minimum $E_m(x_{tot})$. **(b)** Number of open base pairs vs. total distance. Inset shows a detailed view of the stair-shaped character of the curve. **(c)** FDC.

the discontinuous opening of base pairs (i.e. the CUR). In contrast, equation (5) in the main text is an approximation that ignores the sequence dependence. The solution to this approximation are smooth expressions that collect the average behavior of the system over an ensemble of sequences (i.e. realizations of the disorder). Figure S8 shows the approximated solution superimposed on one disorder realization.

3.2. Size distribution of CUR

This section shows the results of the simulation of the toy model introduced in the main text. The distribution of sizes of the CUR depends on the parameters of the model. The aim of this section is to characterize such dependency. Starting from the energy contribution of the model (see Eq. 4 in main text for further details), we generate random realizations and obtain the CUR size distribution for each realization of the disorder. After collecting all the simulated data we obtain the averaged size distribution of the CUR for the chosen

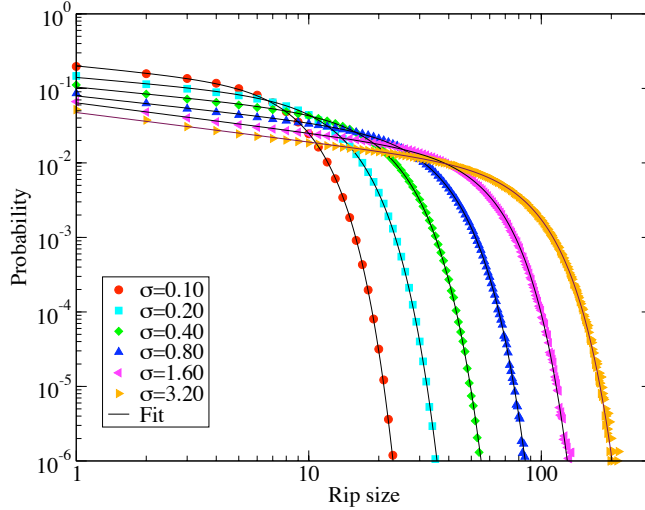


FIG. S9: CUR size distributions for different values of σ . The black curves show the fit of Eq. (6) in main text.

parameters. By varying the parameters of the model along a wide range we observe how the shape of the CUR size distribution changes.

In all our simulations we took $d = 0.59$ nm and $\mu = -1.6$ kcal/mol constant, since the distribution of CUR sizes weakly depends on them. Therefore we only changed σ (the standard deviation of the random distribution of energies) and k (the stiffness of the optical trap). We simulated sequences of 10^4 base pairs and we made 10^4 realizations for each value of σ and k .

3.2.1. Dependence on σ

We fixed the trap stiffness at $k=60$ pN/ μ m. The distribution of CUR obtained for each value of σ is shown in fig S9. The data was fit to Eq. (6) in main text, where a set of 4 parameters (A, B, C, n_c) was obtained for each value of the parameter σ . Fig. S10 shows the dependence of these parameters with σ .

3.2.2. Dependence on k

We fixed the amount of disorder at $\sigma=3.20$ kcal/mol. Figure S11 shows the distribution of CUR for some values of k and their fit to Eq. (6) in main text. Note that in the low k

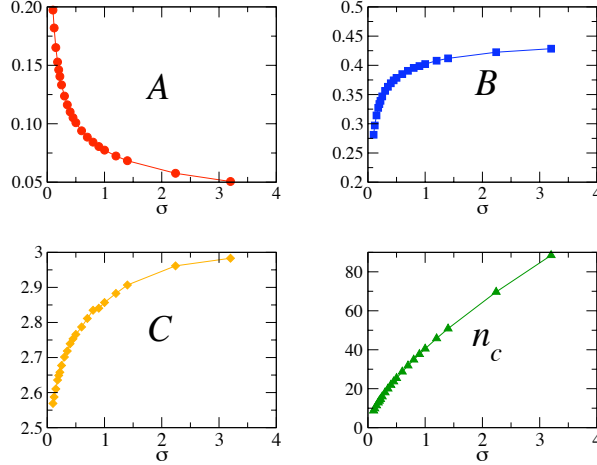


FIG. S10: Fit parameters plotted versus σ .

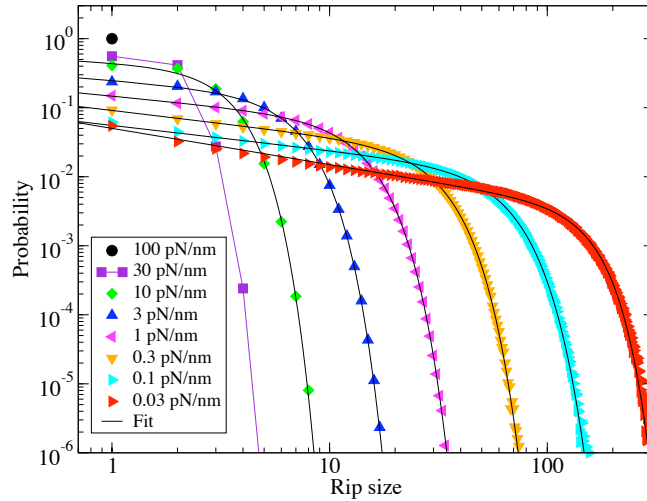


FIG. S11: CUR size distributions for different values of k . The black curves show the fit to Eq. (6) in main text. The tails of the CUR distributions for trap stiffnesses higher than 3 pN/nm need many realizations to be accurately inferred. The distributions are too narrow and the fit of Eq. (3) does not converge easily. Note that at $k = 100$ pN/nm all CUR are one base pair sized.

range the CUR size distributions are wide and have good statistics to extract the values for A, B, C, n_c . However, for $k > 5$ he CUR size distributions are too narrow to be reliably fit to Eq. (6). Figure S12 shows the dependence of the four parameters (A, B, C, n_c) on the trap stiffness.

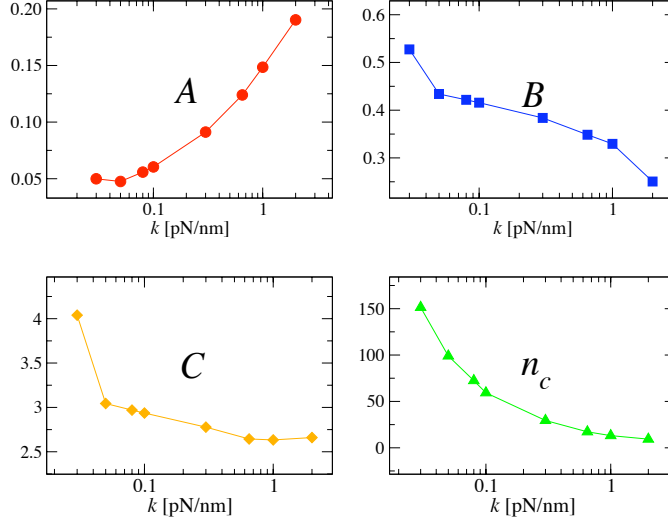


FIG. S12: Fit parameters plotted versus k . The cutoff CUR size (n_c) vs. k follows a power law behavior (see Fig. 3d in main text for a log-log plot).

4. STIFFNESS OF ONE NUCLEOTIDE

Here we calculate the expected stiffness of one nucleotide of ssDNA. The numerical value has been calculated from the elastic response of Freely Jointed Chain (FJC) model for semiflexible polymers, which is given by the following Extension vs. Force curve,

$$x_s(f) = L_0 \left(\coth \left(\frac{bf}{k_B T} \right) - \frac{k_B T}{bf} \right) \quad (1)$$

where x_s is the extension, f is the force applied at the ends of the polymer, L_0 is the contour length, b is the Kuhn length, k_B is the Boltzmann constant and T is the temperature. In the case of a polymer, the contour length (L_0) can be written in terms of the number of monomers (n) times the length of one monomer (d) according to

$$L_0 = n \cdot d \quad (2)$$

In the case of a ssDNA molecule, n is the number of bases and d is the interphosphate distance of one nucleotide. The FJC model assumes that the elastic response of the polymer scales with the number of bases. Therefore, the resulting Extension vs. Force expression is a homogeneous function with respect to the number of bases. The stiffness of the polymer at each stretching force is the derivative of the force with respect to the extension $k_s(f) =$

$df/dx_s = (dx_s/df)^{-1}$. For the FJC model, the stiffness is given by the following expression

$$k_s(f) = \left[n \cdot d \left(-\frac{b}{k_B T} \operatorname{cosech}^2 \left(\frac{bf}{k_B T} \right) + \frac{k_B T}{bf^2} \right) \right]^{-1} \quad (3)$$

Using the parameters from section 2.2.1 ($b = 1.2$ nm, $d = 0.59$ nm) for one nucleotide ($n = 1$) we get a stiffness of $k_s = 113$ pN/nm at $f = 15$ pN and $k_s = 127$ pN/nm at $f = 16$ pN (see Fig. S13).

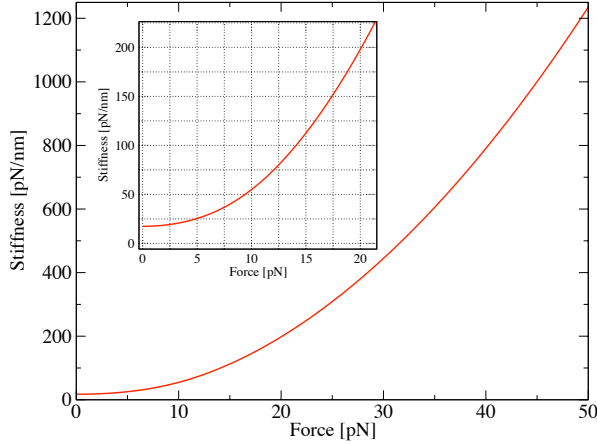


FIG. S13: Stiffness of one nucleotide vs. force. Inset shows a zoomed section of the curve around the unzipping force.

5. PROTEIN-DNA INTERACTION

In the cell, the function of helicases is to unzip DNA during the replication process. Although their mechano-chemistry is not clear [5] we interpret that helicases pull directly on the ssDNA. In this simplified view of the process, we visualize the helicase as a clamp that slides along one strand of the DNA and applies local force at the unzipping fork. In a more general scheme, the helicase applies force on the DNA by means of an effective stiffness $k_{\text{eff}}^{-1} = k_h^{-1} + k_s^{-1}$, where k_h is the stiffness of the helicase and k_s is the stiffness of one base of ssDNA. From the conclusions of our work, we know that k_s is high enough to locally unzip DNA one bp at a time. Therefore, the unzipping process will be one bp at a time as long as k_h is higher than k_s . Indeed, when the helicase pulls directly on DNA the stiffness of the helicase can be assumed to be very large (proteins are indeed very rigid objects) compared

to the stiffness of a single base pair ($k_h^{-1} \ll k_s^{-1}$) and the effective stiffness between the helicase and the DNA is approximately equal to the stiffness of ssDNA ($k_{\text{eff}} \sim k_s$).

The previous explanation can be extended to proteins that interact with DNA. If a protein increases the stiffness of one bp of ssDNA, the local unzipping still could be done one bp at a time. On the other hand, if a protein decreases the ssDNA stiffness below the boundary of $k_s \sim 100$ pN/nm the local unzipping would show CUR of sizes larger than one bp. As far as we know, there is no protein with high compliance bound to the ssDNA between the helicase and the unzipping fork when the replication complex (helicase, polymerase, etc.) is set. However the full scenario of what might happen for different biological models under varied conditions remains to be seen.

6. CUR AND GENES

As an extra information to the reader, here we show the position of the genes that are localized in the two fragments of λ -DNA used in this work. The 2.2 kb fragment contains partially one gene and one complete gene. Upper panel in Fig. S14 shows the localization of the genes along the Force Distance Curve. Lower panel in Fig. S14 shows the position of the genes superimposed on the histogram of number of unzipped base pairs. On the other hand, the 6.8 kb fragment contains partially one gene and 15 complete genes. Figure S15 shows the location of these genes superimposed on the histogram of number of unzipped base pairs. It can be clearly observed that the lengths of most of these genes span over several rips.

We should not expect correlations between the CUR and the genes because the CUR depend on the trap stiffness used in the experimental setup. In other words, a different trap stiffness produces a different distribution of CUR on the same DNA molecule.

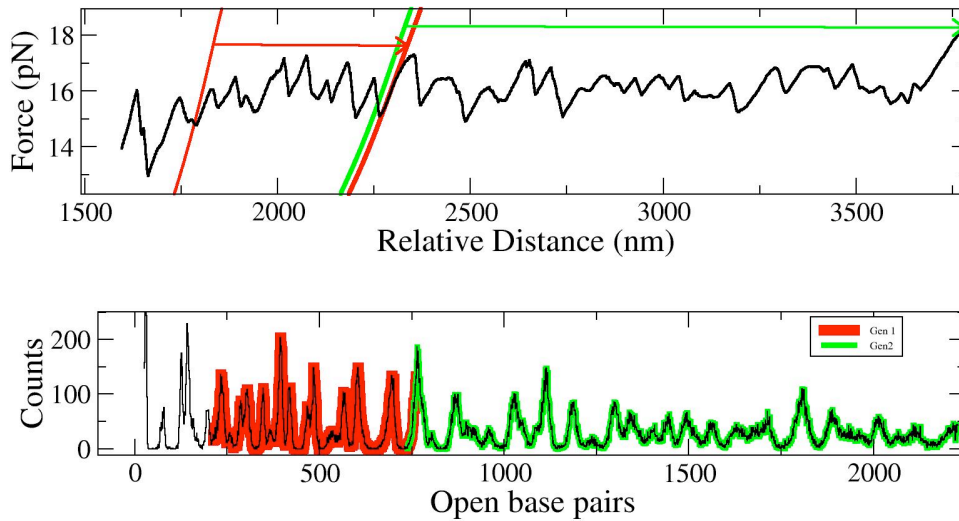


FIG. S14: Localization of genes for the 2.2 kb sequence. **(a)** Start and end points of each gene. The arrow shows the transcription direction. Each gene is depicted in a different color. **(b)** Position of the genes along the histogram of number of unzipped base pairs..

-
- [1] C. Bustamante, J.F. Marko, E.D. Siggia, and S. Smith, *Science* **265**, 1599 (1994).
 [2] S.B. Smith, Y. Cui, and C. Bustamante, *Science* **271**, 795 (1996).
 [3] M.-N. Dessinges, B. Maier, Y. Zhang, M. Peliti, D. Bensimon, and V. Croquette, *Phys. Rev. Lett.*, **89** 248102 (2002).
 [4] D. S. Johnson, L. Bai, B. Y. Smith, S. S. Patel, and M. D. Wang, *Cell* **129**, 1299 (2007).
 [5] T. Lionnet, A. Dawid, S. Bigot, F.-X. Barre, O.A. Saleh, F. Heslot, J.F. Allemand, D. Bensimon, and V. Croquette, *Nucl. Acids Res.* **34** 4232 (2006).
 [6] Available at the NCBI website, <http://www.ncbi.nlm.nih.gov/>

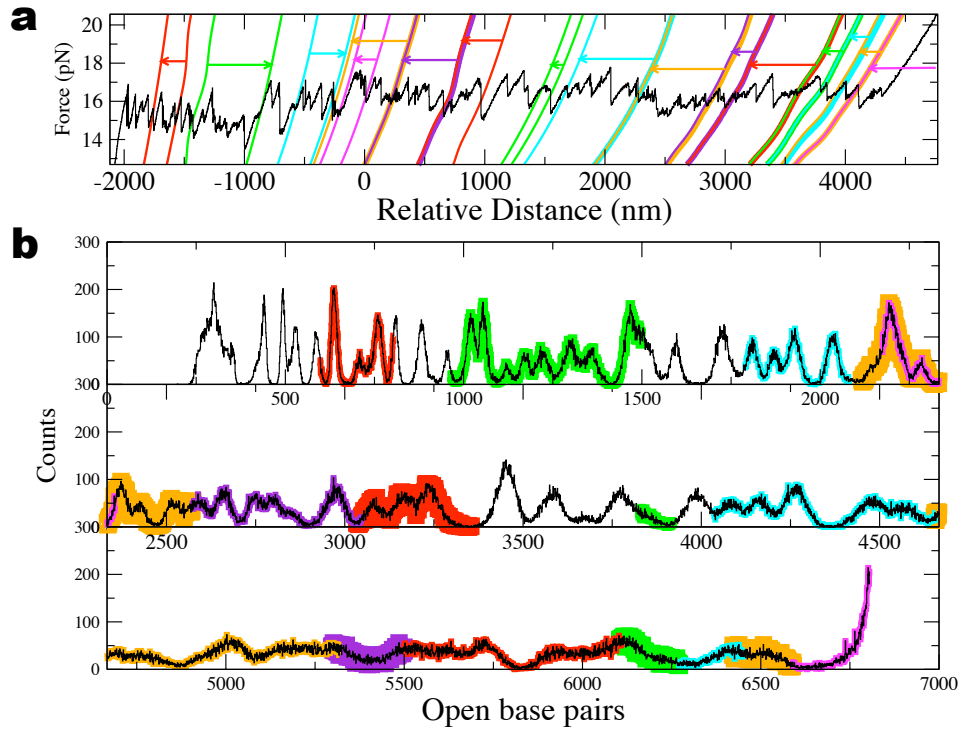


FIG. S15: Localization of genes for the 6.8 kb sequence. Same color code as in Fig. S14.